

An Integer Ambiguity Resolution Procedure for GPS/Pseudolite/INS Integration

HUNG KYU LEE

JINLING WANG

CHRIS RIZOS

*School of Surveying and Spatial Information Systems
The University of New South Wales
Sydney NSW 2052 Australia.*

E-mail: hung.lee@student.unsw.edu.au

Fax: +61-2-9313 7493

Tel: +61-2-9385 4208

Abstract

In order to achieve a precise positioning solution from GPS, the carrier phase measurements with correctly resolved integer ambiguities must be used. Based on the integration of GPS with pseudolites and Inertial Navigation Systems (INS), this paper proposes an effective procedure for single-frequency carrier phase integer ambiguity resolution. With the inclusion of pseudolites and INS measurements, the proposed procedure can speed up the ambiguity resolution process and increase the reliability of the resolved ambiguities. In addition, a recently developed ambiguity validation test, and a stochastic modelling (based on-line covariance matrix estimation) scheme are also adapted to enhance the quality of ambiguity resolution. The results of simulation studies and field experiments indicate that the proposed procedure indeed improves the performance of single-frequency ambiguity resolution in terms of both reliability and time-to-fix-ambiguity.

Key Words: GPS, Pseudolites, INS, Integration, Ambiguity Resolution

1 Introduction

Integrated GPS/INS systems have been developed during the past two decades to overcome the inherent drawbacks of either system. They have been widely used in the fields of aerial photogrammetry, airborne gravimetry, mobile mapping, vehicle navigation, guidance and control (see, e.g., Bevely et al., 2000; Da et al., 1997; Grejner-Brzezinska et al., 1998; Kwon & Jekeli, 2001). Integrated GPS/INS systems can provide a complete navigation solution (position, velocity, and attitude) with improved availability, smoother trajectories, greater integrity and reduced susceptibility to jamming and interference (Farrell & Barth, 1998; Greenspan, 1996).

The performance of existing GPS/INS systems relies heavily on the quality of GPS measurements and the geometry of the satellite constellation. In most airborne applications, however, there are stringent requirements in terms of positioning accuracy, availability and integrity that cannot be entirely met. For example, due to the limited number of GPS satellites, a sufficient number of 'visible' satellites cannot be guaranteed at all times and locations. Even when some low elevation satellites can be tracked, the measurements from these satellites are contaminated by relatively high atmospheric noise. Therefore, this intrinsic shortcoming of satellite-based positioning systems results in, for example, poor accuracy in the vertical

coordinate component, which is about three times worse than that of the horizontal coordinate components. These drawbacks can be addressed using ground-based ‘pseudo-satellite’ augmentation.

‘Pseudo-satellites’, commonly called ‘pseudolites’, are ground-based GPS-like signal transmitters, which can be easily installed wherever they are needed. They therefore offer great flexibility in the augmentation of GPS applications to improve the ‘*open air*’ signal availability, or even replace the GPS satellites constellation for indoor applications. An integrated GPS/INS/pseudolite system would be able to improve system performance under a wide variety of poor operational environments. Such an integration concept has been proposed and tested by the authors (Wang et al., 2001; Lee, 2002; Lee et al., 2002). The new integration scheme can be implemented with three different GPS/pseudolite observations, namely Doppler, pseudo-range, and carrier phase. In order to obtain high accuracy of positioning results, the carrier phase measurements with fixed ambiguities have to be utilised in the system filter update stage. Therefore, ambiguity resolution is a key to high precision GPS/pseudolite/INS applications.

The ambiguity resolution (AR) process consists of two main steps: ‘*ambiguity estimation*’ and ‘*ambiguity validation*’. Whilst the former involves least squares estimates of the integer ambiguities, the latter is concerned with the question of whether one is willing to accept the outcomes of the integer least squares solution. It is well known that AR “on-the-fly” (OTF) for short-range kinematic positioning can be easily accomplished with dual-frequency observations, and under the assumption that the satellite ephemeris error and differential atmospheric delay can be ignored. However, for the single-frequency case it is still a challenge to resolve the ambiguities rapidly and reliably (Han, 1997; Wang et al., 2003).

In this contribution a new single-frequency ambiguity resolution procedure has been proposed for use in GPS/pseudolite/INS systems. The proposed procedure uses single-frequency GPS data together with pseudolite and inertial measurements, making it possible to resolve the ambiguities rapidly and reliably. A more realistic stochastic modelling and a statistically rigorous ambiguity validation test scheme are also adapted to enhance the quality of ambiguity resolution. Results from covariance simulations based on the Ambiguity Dilution of Precision (ADOP) factor are presented to examine some effects of the inclusion of pseudolites and INS on the float ambiguity estimation. In addition, the effects of pseudolite

multipath in a kinematic environment are discussed, and three approaches that can be used to handle the error sources will be suggested to avoid the potential biases in the estimates of real-valued integer ambiguities – which is critical for achieving reliable ambiguity resolution. Finally, the results from the field experiments will be presented to demonstrate the effectiveness of the proposed procedure with respect to different operational conditions.

2. An ambiguity resolution aided with pseudolites and Inertial Navigation System (INS)

This section describes a proposed scheme for integer ambiguity resolution based on double-differenced (DD) GPS/pseudolite carrier phase and pseudo-range measurements from single-frequency receivers, and an Inertial Navigation System (INS). Figure 1 outlines the proposed procedure.

2.1 Measurement modelling

Single-frequency GPS DD carrier phase and pseudo-range observables for short baseline applications such as those considered in this paper (<15km) can be defined as follows:

$$\nabla\Delta\phi_{GPS} = \frac{1}{\lambda_{L1}}\nabla\Delta\rho + \nabla\Delta N + \nabla\Delta\varepsilon_{\phi} \quad (1a)$$

$$\nabla\Delta R_{GPS} = \nabla\Delta\rho + \nabla\Delta\varepsilon_R \quad (1a)$$

where λ_{L1} is the wavelength of the L1 GPS carrier phase measurement, $\nabla\Delta\rho$ is the DD true geometric distances, $\nabla\Delta N$ is the DD integer ambiguities, $\nabla\Delta\varepsilon_{\phi}$ and $\nabla\Delta\varepsilon_R$ are the remaining measurement noise for DD carrier phase and pseudo-range, respectively.

In a manner similar to the GPS satellite measurements, the pseudolite DD carrier phase and pseudo-range observables for the short baseline case are:

$$\nabla\Delta\phi_{PL} = \frac{1}{\lambda_p}\nabla\Delta\rho + \nabla\Delta N + \frac{1}{\lambda_p}\nabla\Delta T_p + \frac{1}{\lambda_p}\nabla\Delta d + e_{\phi} \quad (2a)$$

$$\nabla\Delta R_{PL} = \nabla\Delta\rho + \nabla\Delta T_p + \nabla\Delta d + e_R \quad (2b)$$

where λ_p is the wavelength of the carrier frequency; $\nabla\Delta T$ is the DD tropospheric delay; and $\nabla\Delta d$ is the pseudolite location error.

In the above equations (1) and (2) it is necessary to note that the pseudolite location error and tropospheric delay cannot be removed even though the double-differencing technique is applied. The reason for this is that pseudolites are much closer to the user receivers than the satellites are. However, the optimal locations of pseudolites can minimise the impact of pseudolite location errors on the measurement model and on the positioning solutions (Wang & Lee, 2002). The tropospheric delay can be significantly mitigated through applying a model, which is suitable for the pseudolite observations (Hein, 1997; Dai, 2002).

Strapdown-INS sensors (e.g. accelerometers, and gyroscopes) output three components of the specific force vector and three components of the angular velocity vector in the *body* frame, denoted by f^b and ω_{ib}^b , respectively. Whilst the subscripts of the angular velocity vector indicate the direction of the rotation, the superscript represents the frame in which the vector is expressed. In this case, angular velocity of the *body* frame with respect to the *inertial* frame is defined in the *body* frame. The specific forces and angular velocities can be used to determine all parameters required for trajectory determination, such as position, velocity and attitude, by solving the following system of differential equations (see, e.g., Wong, 1988; Farrell & Barth, 1998, Savage, 2000):

$$\dot{r}^n = -\Omega_{en}^n r^n + v^n \quad (3a)$$

$$\dot{v}^n = R_b^n f^b - (\Omega_{en}^n + 2\Omega_{ie}^n) v^n + g^n \quad (3b)$$

$$\dot{R}_b^n = R_b^n \Omega_{ib}^b - \Omega_{in}^n R_b^n \quad (3c)$$

where \dot{r}^n , \dot{v}^n , \dot{R}_b^n are the time derivatives of the position vector, the velocity vector, and the rotation matrix between body and navigation frame, respectively.

To solve equation (3), the sensed observations f^b and ω_{ib}^b , as well as the gravity vector (g^n), and the Earth rotation rate (ω_{ie}^n), are needed. The observations can be identified on the right-

hand side of the equations, where the angular velocity vector is contained in Ω_{ib}^b , a skew-symmetric matrix. The solution and numerical implementation of the above differential equation is discussed in *ibid*. Considering the position component, the INS delivers three-dimensional position at i_{th} epoch:

$$r_i(-) = r_{i-1}(+) + \Delta r \quad (4)$$

where $r_{i-1}(+)$ is the filter-updated position at $i-1_{st}$ epoch, and Δr is the position increments obtained from integrating equation (3) between two consecutive epochs.

Linearisation of the DD GPS/pseudolite observation equations with the INS-predicted antenna positions yields the following expression:

$$L = AX + V \quad (5)$$

where L is the measurement vector, A is the design matrix, and V is the residual vector:

$$A = \begin{bmatrix} A_b & \lambda_1 I_{m \times m} \\ A_b & \mathbf{0}_{m \times m} \\ I_{3 \times 3} & \mathbf{0}_{3 \times m} \end{bmatrix} \quad (6a)$$

$$X = \begin{bmatrix} X_b \\ X_a \end{bmatrix} \quad (6b)$$

$$L = \begin{bmatrix} \nabla \Delta \phi - \nabla \Delta \rho_0 \\ \nabla \Delta R - \nabla \Delta \rho_0 \\ r_{i-1}(+) + \Delta r - r_0 \end{bmatrix} \quad (6c)$$

where A_b is the $m \times 3$ DD design matrix that contains information on the relative receiver-satellite geometry, X_b is the 3-vector of the unknown increments of the three-dimensional baseline components, and X_a is the m -vector of the real-valued unknown DD integer ambiguities. $\nabla \Delta \phi$, $\nabla \Delta R$, and $\nabla \Delta \rho_0$ are the m -vector of the DD GPS/pseudolite carrier phase and pseudo-range measurements and the DD geometric distance, respectively (computed with respect to an approximate antenna position r_0).

A corresponding covariance matrix for the observation equation can be written:

$$Q_l = \sigma_0^2 \begin{bmatrix} Q_{\nabla\Delta\phi} & 0 & 0 \\ 0 & Q_{\nabla\Delta R} & 0 \\ 0 & 0 & Q_{\Delta r} \end{bmatrix} \quad (7)$$

where $Q_{\nabla\Delta\phi}$ and $Q_{\nabla\Delta R}$ is the $m \times m$ cofactor matrix for the DD GPS/pseudolite carrier phase and pseudo-range observations respectively, and $Q_{\Delta r}$ is the 3×3 cofactor matrix for the INS positioning solution, which is obtained from the position component of the covariance matrix $Q_{i_{GPS/INS}}(-)$ of the predicted states as follows:

$$Q_{i_{GPS/INS}}(-) = \Phi_{i,i-1} Q_{i-1_{GPS/INS}}(+)\Phi_{i,i-1}^T + R_{i-1} \quad (8)$$

where $\Phi_{i,i-1}$ is the Kalman filter transition matrix, $Q_{i-1_{GPS/INS}}(+)$ is the Kalman filter-updated covariance matrix at $i-1_{st}$ epoch, and R_{i-1} is the system noise matrix.

Stochastic modelling, which determines the values of equation (7), is a crucial step for AR (Wang, 1999). Q_{ins} matrix can be obtained from the system integration filter (e.g. equation (8)). An on-line stochastic estimation scheme for GPS and pseudolite (PL) observations based on post-fit residuals is adapted in this procedure to determine $Q_{\nabla\Delta R}$ and $Q_{\nabla\Delta\phi}$. A realistic covariance matrix for the observations can be estimated based on the residual series from previous epochs as follows (*ibid*):

$$Q_{\nabla\Delta\phi,R} = Q_{\hat{V}_{GPS/PL}} + A_{GPS/PL} Q_{\hat{X}} A_{GPS/PL}^T = \frac{1}{N} \sum_{k=1}^N \hat{V}_{i-k} \hat{V}_{i-k}^T + A_{i_{GPS/PL}} Q_{\hat{X}_i} A_{i_{GPS/PL}}^T \quad (9)$$

where $Q_{\hat{V}_{GPS/PL}}$ is the covariance matrix for the residuals of GPS/PL measurements, $A_{GPS/PL}$ is the design matrix that contains line-of-sight vectors for GPS/pseudolite, $Q_{\hat{X}}$ is the covariance matrix for the unknown parameters, i denotes the current epoch, and N is the width of the moving data ‘window’ (Wang, 1999).

Special attention should be paid to the selection of the window width. According to *ibid*, an optimal width of the window is in the range of 10-30 epochs with 1-second sampling rate. One of the main benefits of this approach is that it is unnecessary to separately model satellite and pseudolite measurements. Using the estimated covariance matrix for the observations, the precision of the estimation results can be improved, and therefore a better AR performance can be expected.

2.2 Integer ambiguity estimation

The integer ambiguity estimation is performed in two steps: a) real-valued (float) ambiguities are estimated, and b) the best integer ambiguity combination is validated. Based on the least squares principle, the estimates of the unknown parameters \hat{X} in equation (5) can be obtained:

$$\hat{X} = (A^T P A)^{-1} A^T P L, \quad (10)$$

$$Q_{\hat{X}} = (A^T P A)^{-1} = \begin{bmatrix} Q_{\hat{X}_b} & Q_{\hat{X}_b \hat{X}_a} \\ Q_{\hat{X}_a \hat{X}_b} & Q_{\hat{X}_a} \end{bmatrix} \quad (11)$$

$$V = L - A \hat{X} \quad (12)$$

$$\hat{s}_0^2 = \frac{\Omega_0}{m}, \quad (13)$$

with

$$\Omega_0 = V^T P V = L^T P L - L^T P A \hat{X}$$

where $\hat{X} = (\hat{X}_b, \hat{X}_a)^T$; \hat{X}_b and \hat{X}_a is the baseline and the real-valued (float) ambiguity vector, $Q_{\hat{X}}$ is the cofactor matrix of the estimated unknown parameters, V is the least squares residual vector, and \hat{s}_0^2 is the *a posteriori* variance cofactor.

After estimating the float ambiguities, a search procedure will be performed to obtain the integer-valued ambiguities. The Least squares AMBiguity Decorrelation Adjustment (LAMBDA) method (Teunissen, 1993) is used for this purpose. The main feature of the method is the decorrelation of the ambiguities via the Z-transformation. If the ambiguity

elements \hat{X}_a are fixed to the integer values \tilde{X}_a , the ambiguity-fixed baseline solution can be obtained:

$$\tilde{X}_b = \hat{X}_b - Q_{\hat{X}_b, \hat{X}_a} Q_{\hat{X}_a}^{-1} (\hat{X}_a - \tilde{X}_a) \quad (14)$$

$$Q_{\tilde{X}_b} = Q_{\hat{X}_b} - Q_{\hat{X}_b} Q_{\hat{X}_a}^{-1} Q_{\hat{X}_a, \hat{X}_b} \quad (15)$$

and

$$\tilde{\Omega}_0 = \Omega_0 + (\hat{X}_a - \tilde{X}_a)^T Q_{\hat{X}_a}^{-1} (\hat{X}_a - \tilde{X}_a) \quad (16)$$

2.3 Ambiguity validation

When one or more integer ambiguity combinations are accepted in the process of ambiguity search, the integer ambiguity combination resulting in the minimum quadratic form of the least squares residuals (equation (16)) will be considered as the most likely (best) solution. However, it is crucial to ensure that the most likely integer ambiguity combination is statistically better than the second best combination as defined by the second minimum quadratic form of the least squares residuals. This is called the '*ambiguity validation test*'.

A recently developed validation test scheme is implemented to overcome the drawback of the traditional method (F-ratio test), for which the probability distribution is unknown. The procedure is based on the ratio (called the *W*-ratio) of the difference between the minimum and second minimum quadratic forms of the least squares residuals and its standard deviation. The *W*-ratio value can be defined as (Wang et al., 1998):

$$W = \frac{d}{\hat{s}_0 \sqrt{Q_d}} \quad (17)$$

where

$$d = \tilde{\Omega}_{0(second)} - \tilde{\Omega}_{0(first)} \quad (18)$$

$$Q_d = (\tilde{X}_{a(second)} - \tilde{X}_{a(first)})^T Q_{\tilde{X}_a}^{-1} (\tilde{X}_{a(second)} - \tilde{X}_{a(first)}) \quad (19)$$

where Q_d is the cofactor of d , and s_0^2 is the *a posteriori* variance. In this situation, the W-ratio has a Student's t -distribution. A critical value for the test statistic is determined based on the given test confidence level and the level of redundancy.

2.4 Discussion on the proposed approach

In order to discuss the effectiveness of the proposed ambiguity resolution procedure which makes use of PL and INS measurements, a covariance matrix for the estimated float ambiguities obtained using single epoch data is derived as follows (*proof*. See Appendix):

$$Q_{\hat{x}_a} = \frac{1}{\lambda_1^2} (Q_{\nabla\Delta\phi} + Q_{\hat{r}}) \quad (20)$$

with

$$Q_{\hat{r}} = A Q_{\hat{x}_b} A^T \quad (21a)$$

$$Q_{\hat{x}_b} = (Q_{\hat{x}_b, \nabla\Delta R}^{-1} + Q_{ins}^{-1})^{-1} \quad (21b)$$

where $Q_{\hat{r}}$ is the covariance matrix for the DD range estimate, $Q_{\hat{x}_b}$ is the covariance matrix of the (float) baseline solution, and $Q_{\hat{x}_b, \nabla\Delta R}$ denotes the covariance matrix of the carrier phase-only baseline solution.

Equation (20) is the covariance matrix of the float ambiguities, indicating the precision and correlation characteristics of the estimated float ambiguities. This matrix is influenced by the covariance matrices of the DD carrier phase measurements ($Q_{\nabla\Delta\phi}$) and the DD range estimates ($Q_{\hat{r}}$). In reality, AR performance is dependent on the covariance matrix of the estimated float ambiguities because it defines the ambiguity searching space and the quality of the real-valued ambiguity estimates (Teunissen, 1997). For instance, the search for the integer ambiguities becomes difficult in cases where the float ambiguities are less precise, and are highly correlated as the search space becomes elongated. The search is easier when the ambiguities are more precise and less correlated. Therefore our aim in this contribution is to

improve the covariance matrix of the float ambiguities in terms of its precision and correlation characteristics by improving the precision of the DD range estimates. This is due to the fact that the covariance matrix of the float ambiguity estimates is mainly driven by the precision of the DD range estimates

Now another question arises: ‘How can we improve the precision of the range estimates?’ Equation (21) provides a clue to the answer. First of all, an examination of equation 21a reveals that the covariance matrix for the range estimates is influenced by the geometry of the GPS/pseudolite constellation, and the covariance matrix for the ambiguity float baseline solution. This means that the less correlated and more precise float ambiguities can be obtained if better geometry is used and/or the baseline solution is improved. In the proposed procedure, the former can be achieved using pseudolites signal(s), as the proper inclusion of pseudolites can enhance the geometry (in that the number of satellites tracked is increased, and the line-of-sight vector between epochs changes significantly). On the other hand, the latter can also be achieved by introducing INS-predicted position observations, due to the fact that equation (21b) implies that the baseline solution becomes more precise when using additional measurements. Hence, the use of PL and INS measurements should significantly improve the performance of single-frequency AR process.

3. Simulation Studies

A series of simulation studies based on Ambiguity Dilution of Precision (ADOP) values, which represents both the precision and the correlation characteristics of the estimated ambiguities (Teunissen, 1997), were carried out to investigate the impact of including INS and PL observations on the AR process. In the analyses, a GPS satellite and pseudolite transmitter constellation was generated using a GNSS simulation tool (Lee et al., 2002), while the covariance matrix for the INS-predicted positions was obtained by covariance simulation (Farrell & Barth, 1998). Note that the observation precisions (1σ) of GPS/pseudolite pseudo-range and carrier phase measurements were considered to be 0.3m and 0.005m, respectively. The INS instrument was considered to be of a ‘tactical-grade’ (gyro drift 5 deg/h and accelerometer bias 500 μ g).

Figure 2 depicts the ADOP changes for a 30 second sequential solution as a function of the number of pseudolites used. Note that the INS-predicted positions are also included in the

solutions. As expected, the result reveals that the more pseudolite measurements used, the better the AR performance. It is of interest to note that the ADOP is significantly decreased even if only *one* pseudolite is added to the GPS constellation. However, if more than three pseudolites are used, this does not improve the ADOP values much further.

Another benefit associated with the inclusion of pseudolites in the AR process is the relatively rapid change of the line-of-sight vector, that in turn enhances the performance of the AR process. This is because the relative change in *satellite-receiver geometry* plays a crucial role in AR. In order to investigate such an effect, three different user dynamics, defined by accelerations of 0.1 m/sec², 0.5 m/sec², and 1.0 m/sec² respectively, were considered. It should be noted that the line-of-sight is completely determined by the user's dynamics as the locations of the pseudolites are fixed. Figure 3 illustrates the *vehicle dynamics effect* in AR due to the change in relative pseudolites-receiver geometry. Of course, the overall trend indicates that the higher the dynamics, the smaller the ADOP values (hence enhanced AR performance). However, the performance cannot be improved over time (increased velocity). For instance, the cases with 0.5 m/sec and 1.0 m/sec accelerations become identical at the 30 second epochs, but on the other hand the ADOP difference reaches the maximum value around the 10 second epoch. This may be due to the fact that although the velocity is continuously increasing, the user is getting further away from the pseudolite locations, and thus the relative change of the geometry becomes less.

More analyses were performed to study the impact of including INS-predicted position on the AR procedure. However, an important thing to be considered is the length of time of the assumed GPS/pseudolite signal blockage, because during a blockage an integration filter (typically a Kalman filter) is unable to be updated, resulting in an error growth of the INS-predicted position. The magnitude of the error depends on the length of the blockage and the quality of the INS instrument. Moreover, during the AR procedure the filter cannot be updated by the accurate (ambiguity-fixed) carrier phase solution. These facts were considered in the analyses. Four scenarios, with different signal blockage lengths, were considered: *instantaneous* (normally caused by a cycle slip), 10, 20, and 30 seconds. Figure 4 depicts the influence (on the ADOP value) of introducing the INS-predicted position (and/or pseudolites) into the AR process as a function of the four different scenarios. All of the results, in the case of both GPS/INS and GPS/PL/INS integrated systems, indicate that the inclusion of an INS significantly reduces the ADOP values, and hence improves the AR performance.

Looking into the results in more detail, one can also identify the impact of the different behaviours of INS-predicted position error. The '*Instantaneous*' blockage (the smallest error growth), for both GPS/INS and GPS/PL/INS systems, using single-frequency receivers is indeed superior to that of the dual-frequency GPS-only case. In other words, it appears that single epoch AR could be possible with such integrated systems. In the case of the 10 second blockage, even though the three sets of results (dual-frequency GPS-only, GPS/INS, and GPS/PL/INS) are similar at the beginning, the GPS/PL/INS results are much better than those of GPS/INS. Note that the results from the dual-frequency GPS case are always better than those of the integrated systems in the case of 20 and 30 second blockages. However, although epoch-by-epoch AR with dual-frequency GPS data for short baselines is possible, using GPS/INS and GPS/PL/INS systems can permit the resolution of the ambiguities within a couple of seconds.

Figure 5 illustrates the change of ADOP (and hence the AR performance) as a function of the length of the signal outage. It can be seen from Figure 5 that the ADOP values vary significantly, depending on the magnitudes of the initial position errors. However, those values become similar after a 30 second sequential solution, which means the time-to-fix will be different, depending on the length of the signal blockage. However, the most impressive thing in the results is that aiding from PL and INS measurements would significantly improve the single-frequency AR performance.

In order to solve the problem of position error growth during the AR procedure, one can consider the use of the DD pseudo-range measurements for the Kalman filter update as indicated in Figure 1, once the signals are reacquired. Even though the precision of the pseudo-ranges is not as good as that of carrier phase measurements with correctly fixed ambiguities, pseudo-ranges can be helpful in preventing the errors from increasing exponentially.

Figure 6 depicts the position error changes during the signal blockage (30 seconds). In this case study, the DD pseudo-range measurements are used in the filter update, after the signals are reacquired. The error growth stops and drops down to a certain level, which reflects the level of DD pseudo-range errors.

Figure 7 shows the ADOP changes with and without the use of DD pseudo-range data in the filter updating during the AR procedure. The results indicate that the AR performance will be improved by using pseudo-range measurements. Even though the degree of improvement of the ADOP values is small just after regaining the ranging signals (e.g., at the first epoch in Figure 7), the magnitude does become significant with increasing time elapsed since the first epoch. Therefore this is a useful method to enhance the AR performance after a long signal blockage.

4. Experiment and results

Land vehicle experiments were carried out on 23rd April 2003 at the Clovelly Bay Carpark in Sydney, Australia. The objective of these experiments was to evaluate ambiguity resolution performance of the integrated GPS/pseudolite/INS system based on the proposed procedure.

4.1 General description of the tests

A prototype pseudolite system developed at DSO National Laboratories of Singapore and UNSW was used in the test (Soon et al., 2003). The locations of the pseudolite and the reference station were precisely surveyed using Leica GPS system 500 receivers. During the trial the pseudolite signal was configured to transmit with the power of -10 dB (assigned PRN 12). Two Novatel Millennium receivers with Leica AT504 choke-ring antennas were used at both the reference and rover (vehicle) stations to track the GPS and pseudolite signals. The INS used in this experiment was a Boeing C-MIGITS II, which is considered to be a tactical-grade accuracy unit (5 deg/h, 500 μ g). The antenna and INS were mounted on the roof of the test vehicle. Raw IMU measurements (accelerations and angular velocities) were recorded at 100Hz, while the single-frequency GPS/pseudolite data were logged at 1Hz. During the experiment there were 6 visible satellites (above the cut-off angle of 15°) and one pseudolite (PRN 12). The maximum baseline length between the reference station and the rover was of the order of 50 metres, as shown in Figure 8.

4.2 Special consideration of pseudolite multipath

One of major error sources for PL measurements is multipath. Compared with the multipath from satellite signals, the pseudolite multipath has some unique characteristics (Ford et al., 1996; Dai, 2002). First of all, the pseudolite multipath is not only due to the signals reflected from surfaces, but also from the signal transmitter itself. In addition, the GPS satellites are

orbiting and far away, while on the other hand the pseudolite transmitters are stationary and nearby. Hence, whilst the magnitude of multipath caused by a satellite signal transmitter itself is relatively smaller and slowly changing, that of pseudolite is larger and changes rapidly in the case of a kinematic scenario. If the pseudolite and the receiver were both stationary, the multipath error would be a constant (*ibid*). However, in a kinematic scenario, multipath will not be constant and can significantly increase the noise level of the measurements.

In order to illustrate typical behaviour of GPS and pseudolite multipath in a kinematic mode, DD carrier phase and pseudo-range residuals are shown in Figure 9. Since the DD technique can remove and/or dramatically reduce the common error sources between reference and rover stations in the case of a short baseline, the residual errors can be considered to be mainly composed of multipath. It can be noticed from the results that the pseudolite multipaths (the lower graphs) are slightly biased and show a much higher noise level for both carrier phase and pseudo-range measurements, compared to the residuals from the satellites (the upper graphs). The mean value and the standard deviation of the pseudolite carrier phase data are 0.06 cycles and 0.103 cycles, respectively; and for the pseudo-range data are 0.868m and 1.833 m, respectively. The bias terms seem to be caused by the multipath at the stationary reference station. In addition, the pseudolite multipath pattern appears to be related to the vehicle trajectory or dynamics.

Therefore, special efforts should be employed to mitigate and/or handle the pseudolite-caused multipath. Hence, three different methods are considered here in this study. The first method is to use choke-ring antennas at the reference stations and the rover. The second method is to realistically weight the pseudolite observations, by employing a realistic stochastic model (e.g. equation (9)). The third method is to estimate the multipath effect in the pseudolite pseudo-range using one additional unknown parameter in the least squares solution. It should be noted that the third method would be only applicable when the number of satellites is greater than four. Therefore this method will be of benefit to avoid the model infidelity problem due to the relatively severe multipath in the pseudo-range data.

Figure 10 illustrates the multipath error estimation with two system configurations: GPS/pseudolite and GPS/INS/pseudolite. The values were calculated from a comparison of the residuals in Figure 9. The results indicate that the GPS/INS/pseudolite solution provides more precise estimates.

On the other hand, one may ask the question: ‘Does the inclusion of the new parameter degrade the float ambiguity estimation?’ To answer this question analyses based on the ADOP factor were carried out using the same data set as the test discussed above. Figure 11 illustrates the analysis results with respect to three different methods, such as GPS/INS as well as GPS/PL/INS without/with the inclusion of the new parameter. It can be seen from Figure 11 that the inclusion of the pseudolite is helpful in improving the float solutions (smaller ADOP values), and the ADOP values are almost the same even though the additional unknown parameter is included in the least squares processing. Therefore, it can be concluded that the inclusion of the new unknown parameter does not significantly degrade float ambiguity estimation.

4.3 AR performance analysis

In order to demonstrate the performance of the proposed AR procedure, a comparison between different system configurations was conducted. Three different configurations (GPS-only, GPS/INS, and GPS/pseudolite/INS) were applied for all the data processing in single-epoch solution mode. The AR performance can be evaluated by the comparison of ambiguity validation test statistics (W-ratio) obtained by equation (17), in that the larger values for the statistics the higher the probability of correctly fixing the integer ambiguity (Wang, 1999; Wang et al., 2003).

Figure 12 shows the W-ratio values in the case of using only GPS data, they are mostly less than their critical values (4.5 with 99% confidence level). This means that most of the integer ambiguity combinations cannot be successfully validated. However, the ratios obtained by either integrated GPS/INS or GPS/pseudolite/INS are sufficiently large to validate the correct ambiguity for critical values (3.2 and 3.0 with 99.9% confidence level respectively). Comparing the results from the GPS/INS case with the GPS/pseudolite/INS case, it can be seen that the ratios from the latter are usually larger than those obtained from the former (see also the averaged W-ratios in Figure 12). Therefore the inclusion of PL observations enhances the AR performance. In addition, the successful validation rates for the three different system configurations based on the aforementioned critical values are 0.4%, 97.4%, and 99.3%, respectively. Hence, it has been demonstrated that the proposed procedure based on GPS/pseudolite/INS integration does indeed perform better.

A realistic estimation of measurement covariance matrices provides reliable statistics for AR. In order to clearly demonstrate this fact, the solutions based on the two different types of stochastic model, namely the 'Preset' and 'Estimated', are obtained. The 'Preset' model is based on an apriori assumption of the measurement precision. For the 'Estimated' model, a realistic measurement covariance matrix is estimated using equation (9). Figure 13 depicts the validation test statistics (W-ratios), indicating that the ambiguity validation test statistics with the 'Estimated' measurement covariance matrices are better than those with the 'Preset' measurement covariance matrices. On the other hand, the successful validation rates for the 'Estimated' and 'Preset' are 92.1% and 99.3%, respectively, which demonstrates the AR performance with 'Estimated' model is superior to that of the 'Preset' models.

The capability of the integrated system to recover from complete GPS/pseudolite signal blockages, and return to a positioning solution with correctly resolved ambiguities, is critical to maintaining high system performance. Therefore the impact of including PL and INS observations on the AR performance after complete GPS/pseudolites signal blockage was also investigated. For this test, signal blockages of 2, 5, 10, 20, 30, 40, and 50 seconds with respect to three different locations in the observation files (referred to as Case I, II, and III) are simulated through modifying the RINEX data files. Note that DD pseudo-range measurements are used in the filter update for the AR procedure, and a sequential solution is applied to estimate the initial float ambiguities.

Figure 14 shows the time-to-fix of L1 carrier phase ambiguities after complete GPS/pseudolite signal blockages. The results indicate that the AR performances of both GPS/INS and GPS/PL/INS are similar after a short signal outage (up to 10 seconds). However, the AR performance is significantly improved by including PL measurements from 20 second outage, excepting for 30 second blockage for Case III. Special attention should be paid to 'Case I', because the most significant improvement was obtained. Hence, it is demonstrated from the results that the proposed AR procedure based on GPS/pseudolite/INS integration makes it possible to resolve the ambiguities within a couple of seconds if the outage is relatively short. Moreover, the AR performance can be considerably enhanced even in the case of a blockage of 50 seconds. The different performances among the three cases appears to be caused by the different error growth rates of the INS-predicted positions, satellite geometry and/or measurement errors.

5. Concluding remarks

Ambiguity resolution is one of the most crucial steps in achieving high accuracy positioning results using an integrated GPS/pseudolite/INS system. In this paper an ambiguity resolution procedure which uses GPS, pseudolite and inertial measurements has been proposed, that improves the performance of single-frequency on-the-fly AR. In the proposed procedure, realistic stochastic modelling and statistically rigorous ambiguity validation scheme were adapted to enhance the reliability of ambiguity resolution.

The potential benefits of the procedure have been demonstrated with the derivation of single epoch covariance of float ambiguities within an integrated GPS/pseudolite/INS system. The simulations based on Ambiguity Dilution of Precision (ADOP) values have shown that the PL measurements can play an important role in the proposed AR procedure. Note that the ADOP value can be significantly decreased even if only *one* pseudolite is added to the GPS constellation. The other benefit of including the pseudolite is the relatively rapid change of the line-of-sight vector that enhances the performance of the AR process. In addition, the AR performance can also be improved by the inclusion of the INS measurements.

The experimental results have shown that appropriate stochastic modelling for the satellite and pseudolite measurements is important for enhancing the performance of ambiguity resolution. It is also demonstrated that ‘instantaneous’ resolution is possible if the duration of the signal blockage is up to a couple of seconds. Moreover, even if the signal blockage is up to 50 seconds, the ambiguities can be fixed within a few ten of seconds, depending on satellite/pseudolite geometry and measurement precision.

Acknowledgements

The first author (HKL) is supported in his PhD research by a scholarship funded by the Kwanjeong Educational Foundation of Korea. The authors would like to acknowledge the assistance of Mr. B.H.K Soon, of the DSO Laboratories, Singapore, and Mr. Michael Moore during the experiment and the preparation of this paper.

Appendix

Proof of Equation (20). (Covariance matrix for single epoch float ambiguity estimation within an integrated GPS/pseudolite/INS system)

From equation (11), we can obtain:

$$\begin{aligned}
A^T P A &= \begin{bmatrix} A_b^T & A_b^T & I \\ \lambda I & 0 & 0 \end{bmatrix} \begin{bmatrix} P_{\nabla\Delta\phi} & 0 & 0 \\ 0 & P_{\nabla\Delta R} & 0 \\ 0 & 0 & P_{ins} \end{bmatrix} \begin{bmatrix} A_b & \lambda I \\ A_b & 0 \\ I & 0 \end{bmatrix} \\
&= \begin{bmatrix} N_{11} & N_{12} \\ N_{21} & N_{22} \end{bmatrix}
\end{aligned} \tag{A1}$$

with

$$N_{11} = A_b^T P_{\nabla\Delta\phi} A_b + A_b^T P_{\nabla\Delta R} A_b + P_{ins}$$

$$N_{12} = \lambda A_b^T P_{\nabla\Delta\phi}$$

$$N_{21} = \lambda P_{\nabla\Delta\phi} A_b$$

$$N_{22} = \lambda^2 P_{\nabla\Delta\phi}$$

Then, the covariance matrix for the unknown parameters is:

$$\mathcal{Q}_{\hat{x}} = \begin{bmatrix} \mathcal{Q}_{X_b} & \mathcal{Q}_{X_b} \mathcal{Q}_{X_a} \\ \mathcal{Q}_{X_a} \mathcal{Q}_{X_b} & \mathcal{Q}_{X_a} \end{bmatrix} = \begin{bmatrix} N_{11} & N_{12} \\ N_{21} & N_{22} \end{bmatrix}^{-1} \tag{A2}$$

According to the matrix inversion by partitioning theorem (Mikhail, 1976), the covariance matrix of the float baseline solution (A3) and of the float ambiguities (A4) are derived as follows:

$$\begin{aligned}
\mathcal{Q}_{X_b} &= \left(N_{11} - N_{12} N_{22}^{-1} N_{21} \right)^{-1} \\
&= \left(\begin{array}{c} A_b^T P_{\nabla\Delta R} A_b + P_{ins} \\ \mathcal{Q}_{\hat{x}, \nabla\Delta\phi}^{-1} \end{array} \right)^{-1} \\
&= \left(\mathcal{Q}_{\hat{x}, \nabla\Delta R}^{-1} + \mathcal{Q}_{ins}^{-1} \right)^{-1}
\end{aligned} \tag{A3}$$

with

$$\begin{aligned}
N_{12} N_{22}^{-1} N_{21} &= \left(\lambda A_b^T P_{\nabla\Delta\phi} \right) \left(\frac{1}{\lambda^2} \mathcal{Q}_{\nabla\Delta\phi} \right) \left(\lambda P_{\nabla\Delta\phi} A_b \right) \\
&= A_b^T P_{\nabla\Delta R} A_b
\end{aligned}$$

$$\begin{aligned}
Q_{X_a} &= N_{22}^{-1} + N_{22}^{-1} N_{21} \underbrace{\left(N_{11} - N_{12} N_{22}^{-1} N_{21} \right)^{-1}}_{Q_{\hat{x}_b}} N_{12} N_{22}^{-1} \\
&= \frac{1}{\lambda^2} Q_{\nabla\Delta\phi} + \frac{1}{\lambda^2} \underbrace{A_b Q_{\hat{x}_b} A_b^T}_{Q_r} \\
&= \frac{1}{\lambda^2} (Q_{\nabla\Delta\phi} + Q_r)
\end{aligned} \tag{A4}$$

with

$$\begin{aligned}
N_{22}^{-1} N_{21} &= \left(\frac{1}{\lambda^2} Q_{\nabla\Delta\phi} \right) (\lambda P_{\nabla\Delta\phi} A_b) \\
&= \frac{1}{\lambda} A_b
\end{aligned}$$

$$\begin{aligned}
N_{12} N_{22}^{-1} &= (\lambda A_b^T P_{\nabla\Delta\phi}) \left(\frac{1}{\lambda^2} Q_{\nabla\Delta\phi} \right) \\
&= \frac{1}{\lambda} A_b^T
\end{aligned}$$

References

Bevly DM, Rekow A, Parkinson B (2000) Comparison of INS vs. carrier-phase DGPS for attitude determination in the control of off-road vehicles. *Navigation*, Journal of the U.S. Institute of Navigation, 47, 257-265.

Dai L (2002) *Augmentation of GPS with GLONASS and Pseudolite Signals for Carrier Phase-Based Kinematic Positioning*. Ph.D Dissertation, School of Surveying and Spatial Information systems, The University of New South Wales, Sydney, Australia.

Da R (1997) Investigation of a low-Cost and high-accuracy GPS/IMU system. *ION National Technical Meeting*, Santa Monica, California, 14-16 January, 955-963.

De Jonge PJ, Tiberius CCJM (1994) The LAMBDA method for integer ambiguity estimation : implementation aspects. Delft Geodetic Computing Centre LGR Series, 12, Delft University of Technology, The Netherlands.

Farrell RA , Barth M (1998) *The Global Positioning System & Inertial Navigation and Integration*. McGraw-Hill, New York.

Ford T, Neumann J, Tos N, Petersen W, Anderson C, Fenton P, Holden P, Barltrop D (1996) HAPPI-a High Accuracy Pseudolite/GPS Positioning Integration. *9th Int. Tech. Meeting of the Satellite Division of the U.S. Inst. of Navigation*, Kansas City, Missouri, 17-20 September, 1719-1728.

Grejner-Brzezinska D, Da R, Toth C (1998) GPS error modeling and OTF ambiguity resolution for high-accuracy GPS/INS integrated system. *Journal of Geodesy*, **72**, 626-638.

Greenspan, RL (1996) GPS and Inertial Integration, B. Parkinson and J.J. Spilker, Jr., eds., *Global Positioning System: Theory and Applications*, volume 2, chapter 7, American institute of Aeronautics and Astronautics, Inc., Washington D.C., USA.

Han S (1997) *Carrier Phase-Based Long-Range GPS Kinematic Positioning*. Ph.D Dissertation, School of Surveying and Spatial Information Systems, The University of New South Wales, Sydney, Australia.

Hein GW, Eissfeller B, Werner W, Ott B, Elrod BD, Barltrop KJ, Stafford JF (1997) Practical investigations on DGPS for aircraft precision approaches augmented by pseudolite carrier phase tracking. *10th Int. Tech. Meeting of the Satellite Division of the U.S. Inst. of Navigation*, Kansas City, Missouri, 16-19 September, 1851-1960.

Kwon JH, Jekeli C (2001) A new approach for airborne vector gravimetry using GPS/INS. *Journal of Geodesy*, **74**, 690-700.

Lee HK, Wang J, Rizos C, Grejner-Brzezinska D (2002) GPS/pseudolite/INS integration: Concept and first tests. *GPS Solutions*, **6**(1-2), 34-46.

Lee HK (2002) GPS/pseudolite/SDINS integration approach for kinematic applications. *15th Int. Tech. Meeting of the Satellite Division of the U.S. Inst. of Navigation*, Portland, Oregon, 24-27 September, 1464-1473.

Soon BHK, Poh EK, Barnes J, Lee HK, Zhang J, Lee HK, Rizos C (2003) Preliminary results of the carrier-smoothed code-phase differential GPS/pseudolite system. *6th Int. Symposium on Satellite Navigation Technology Including Mobile Positioning & Location Services*, Melbourne, Australia, 22-25 July.

Teunissen PJG (1993) A new method for fast carrier phase ambiguity estimation. *IEEE Position, Location and navigation Symposium PLANS 94*, Las Vegas, Nevada, 11-15 April, 562-573.

Teunissen, PJG (1997) A canonical theory for short GPS baselines (Part I-IV). *Journal of Geodesy*, **71**, 320-336, 389-401.

Wang J, Stewart MP, Tsakiri M (1998) A discrimination test procedure for ambiguity resolution on-the-fly. *Journal of Geodesy*, **72**, 644-653.

Wang J (1999) Stochastic modeling for real-time kinematic GPS/GLONASS positioning. *Navigation*, Journal of U.S. Institute of Navigation, **46**, 297-305.

Wang J, Dai L, Tsujii T, Rizos C, Grejner-Brzezinska D, Toth C (2001) GPS/INS/pseudolites: Concepts, simulation and testing. *14th Int. Tech. Meeting of the Satellite Division of the U.S. Inst. of Navigation*, Salt Lake City, Utah, 11-14 September, 2708-2715.

Wang J, Lee HK (2002) Impact of pseudolite location errors in positioning. *Geomatics Research Australasia*, 77, 81-94.

Wang J, Lee HK, Hewitson S, Rizos C, Barnes J (2003) Sensitivity analysis for GNSS integer carrier phase ambiguity validation test. *XXIIIth General Assembly of the IUGG*, Sapporo, Japan, 30 June - 11 July.

Wong RVC (1998) *Development of a RLG Strapdown Inertial Survey System*. Ph.D Dissertation, Department of Geomatics Engineering, The University of Calgary, Canada.

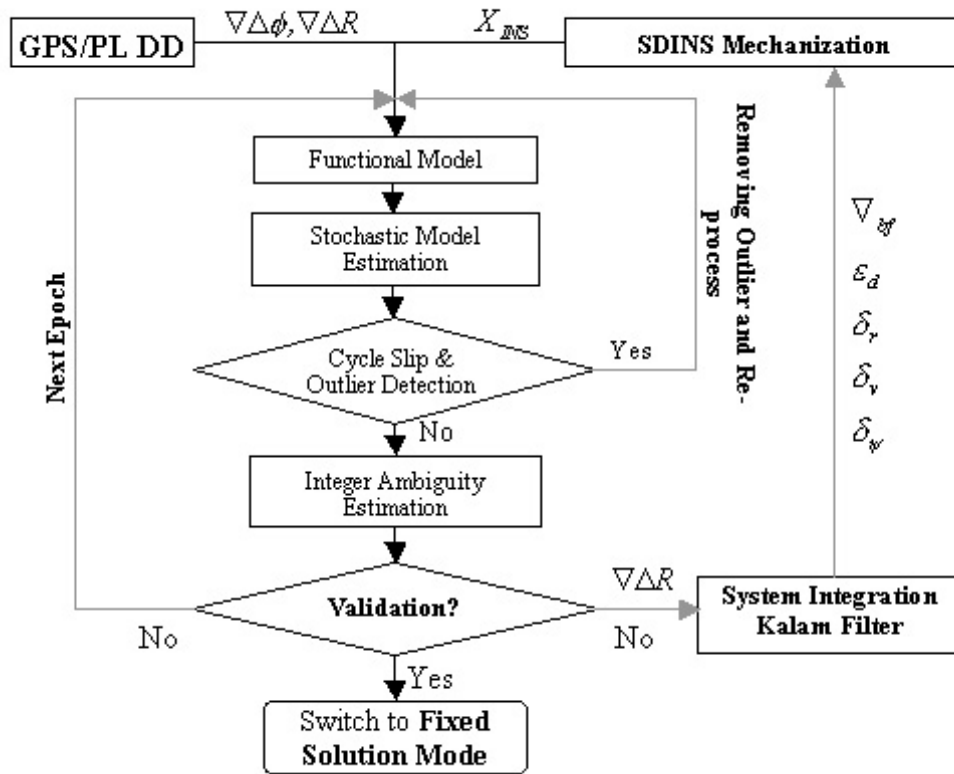


Fig. 1. The proposed ambiguity resolution procedure

where $\nabla\Delta\phi$ and $\nabla\Delta R$ is DD carrier-phases and pseudo-ranges; X_{INS} is the INS predicted-position; $\nabla_{bf}, \varepsilon_d, \delta_r, \delta_v$ and δ_ψ are the filter states (errors of sensors and navigation solutions)

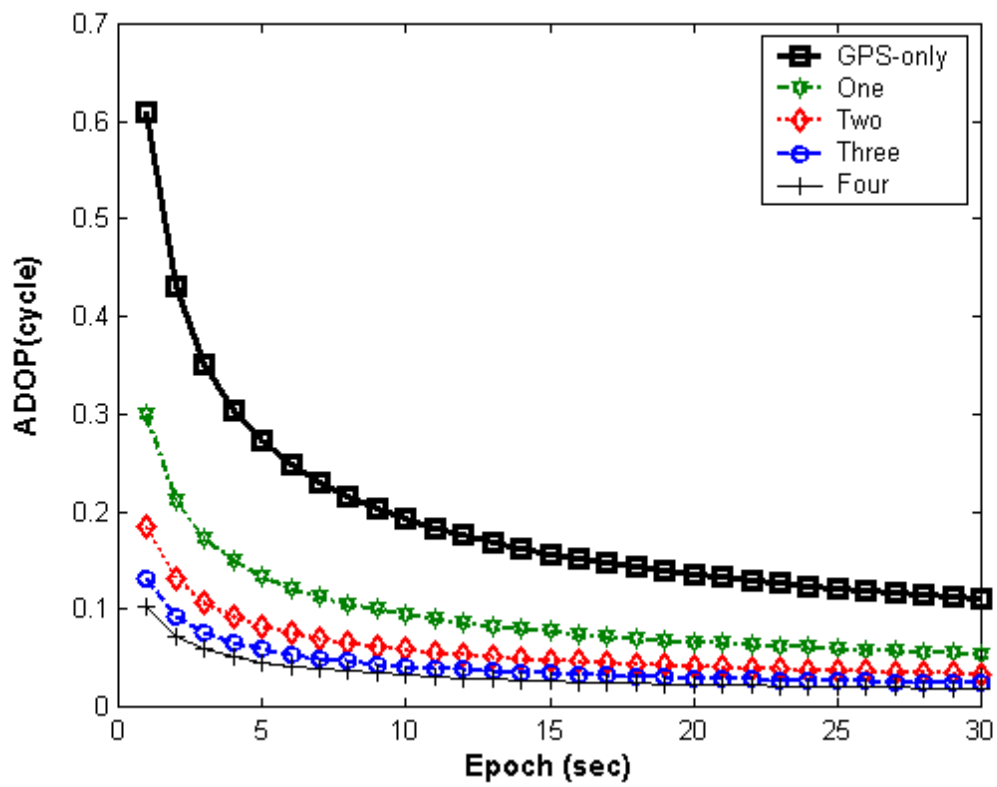


Fig. 2. Impact of Pseudolites on the ADOP (depending on the number of Pseudolites)

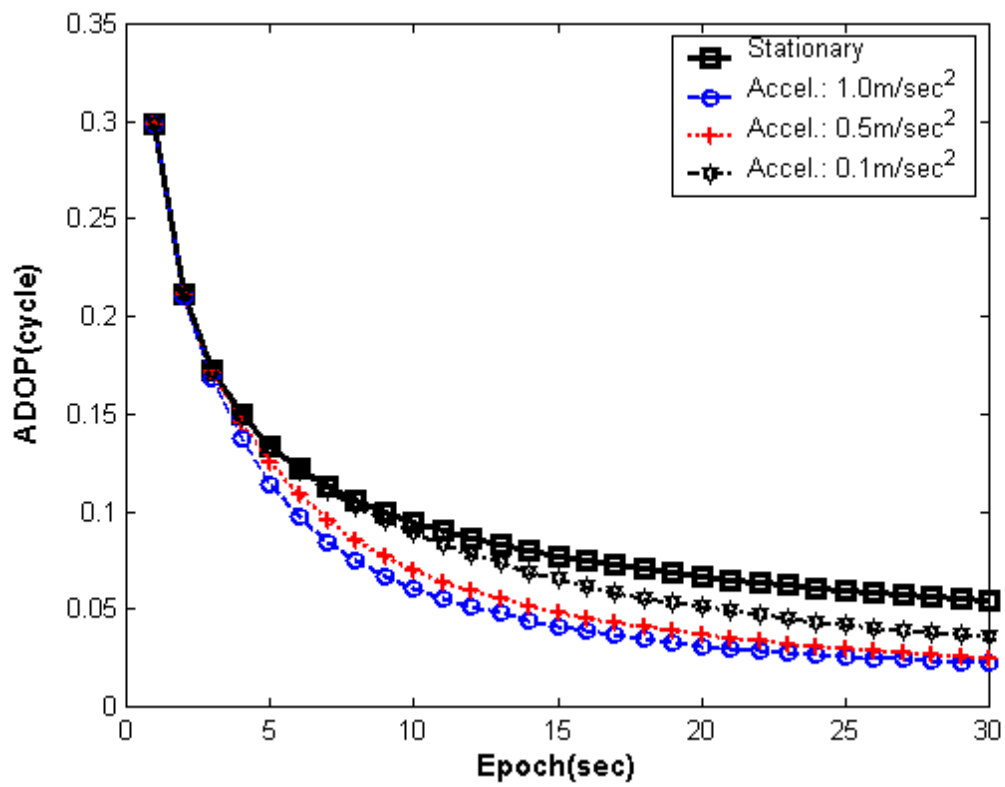


Fig. 3. Impact of Pseudolites on ADOP (depending on the vehicle dynamics)

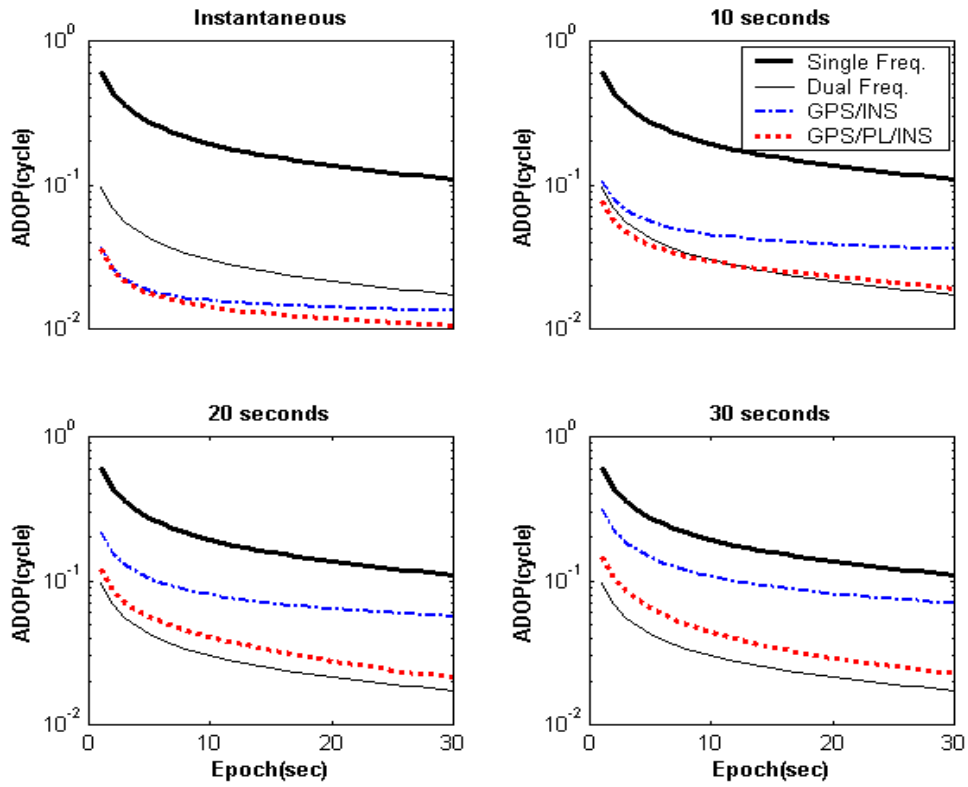


Fig. 4. Impact of INS-predicted position on ADOP (comparison between GPS/INS and GPS/PL/INS systems)

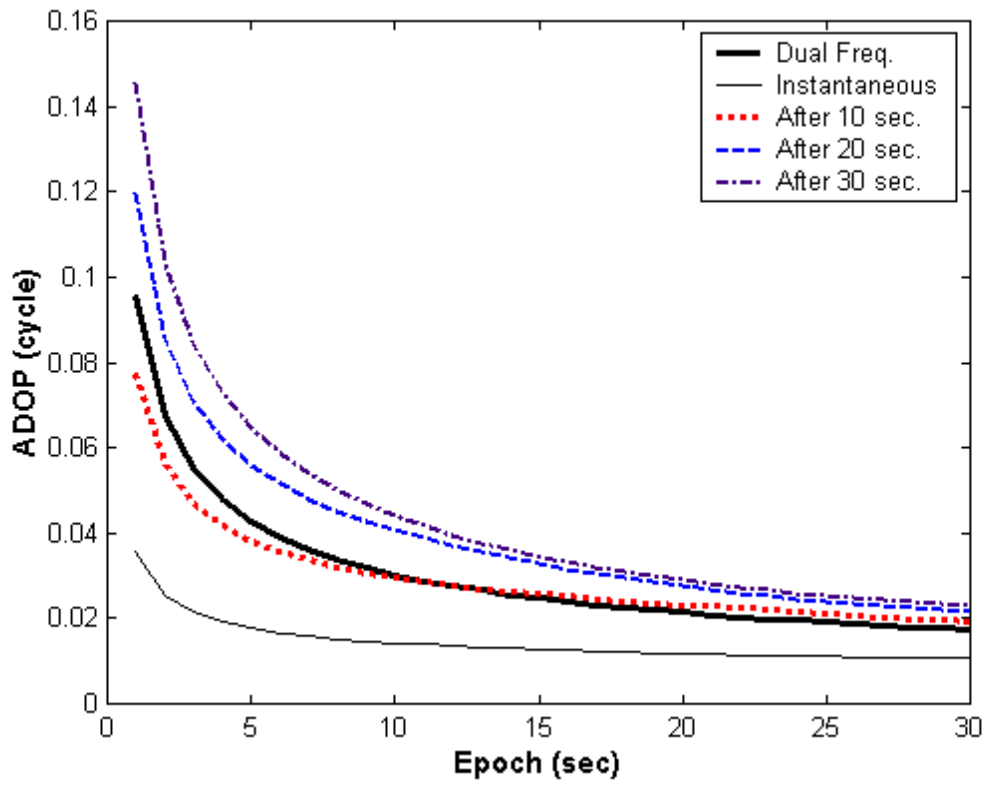


Fig. 5. Impact of INS-predicted position errors bas on ADOP during signal blockages (GPS/PL/INS Systems)

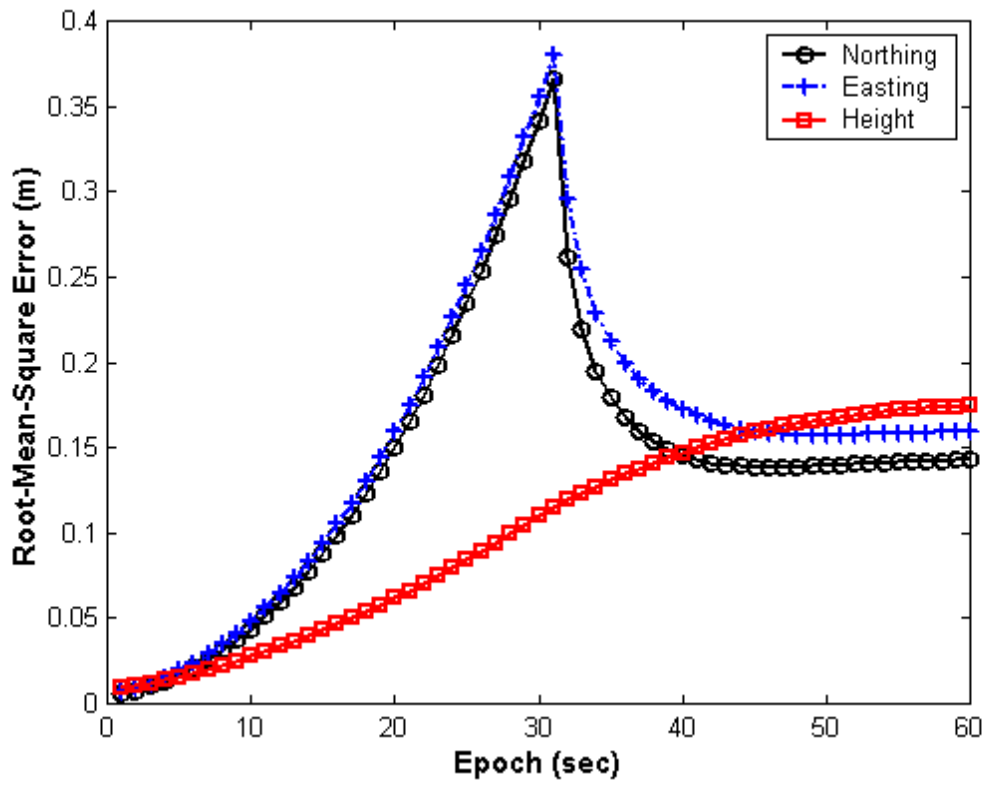


Fig. 6. INS-predicted position error behaviours during absolute signal outage (30 seconds) and updating the filter by the DD pseudo-ranges in the AR procedure.

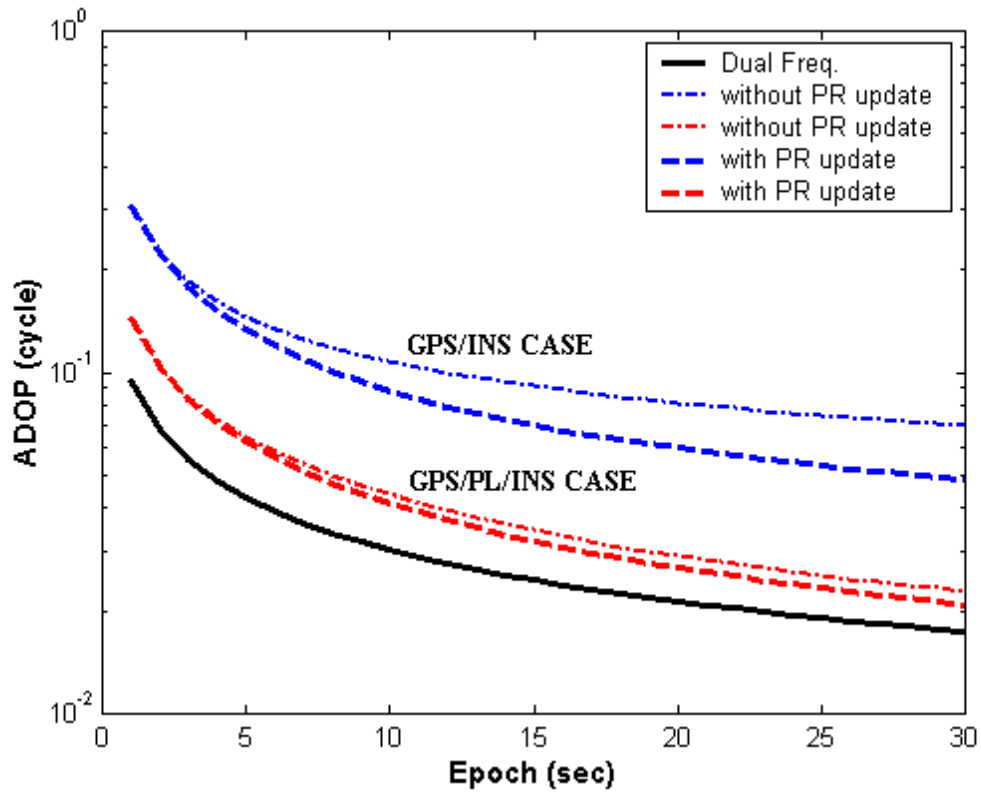


Fig. 7. Impact of updating Kalman filter by DD pseudo-ranges on ADOP after 30 second signal blockage.

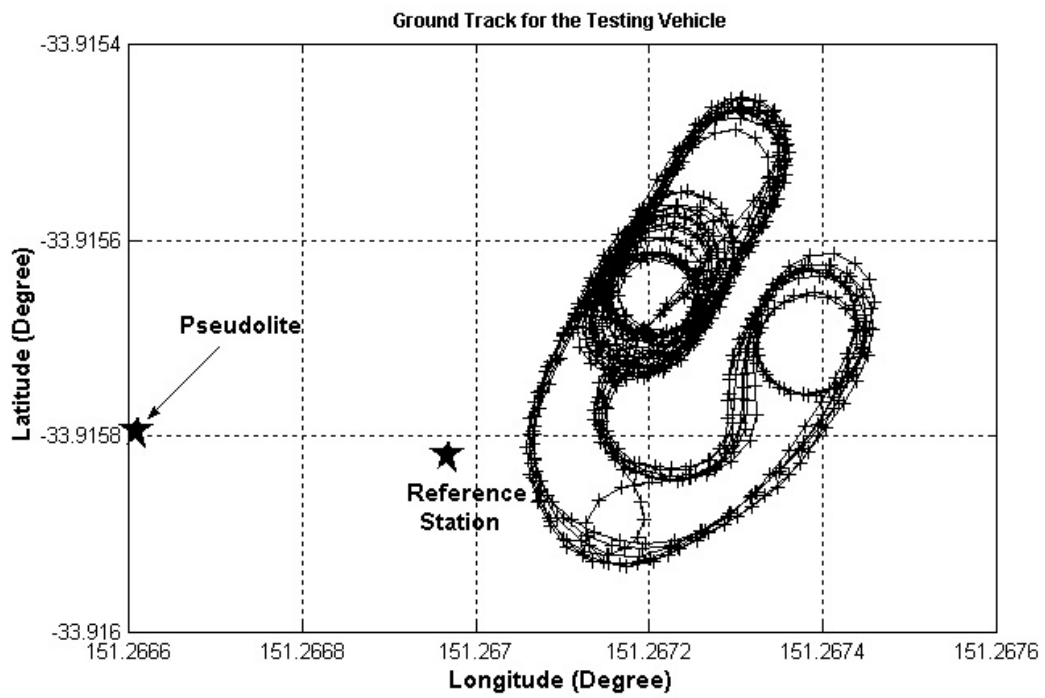


Fig. 8. Vehicle trajectory and locations of reference station and pseudolite

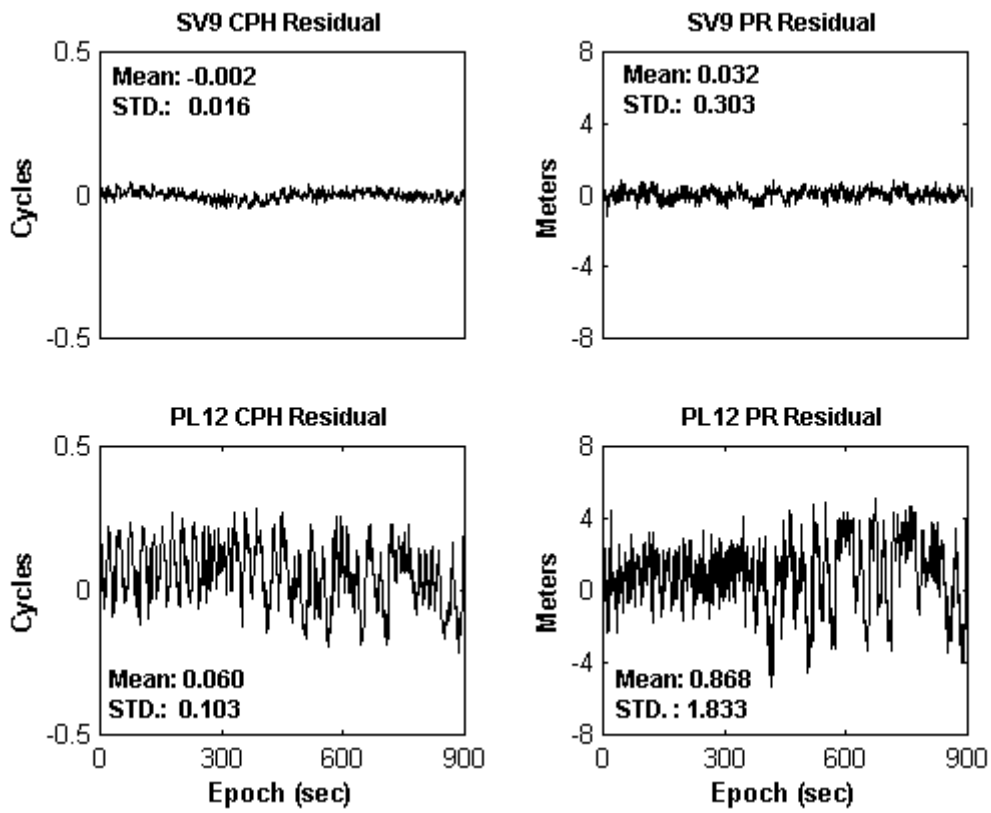


Fig. 9. Multipath influence on the DD GPS/pseudolite observations (Pseudo-Range (PR) and Carrier Phase (CPH))

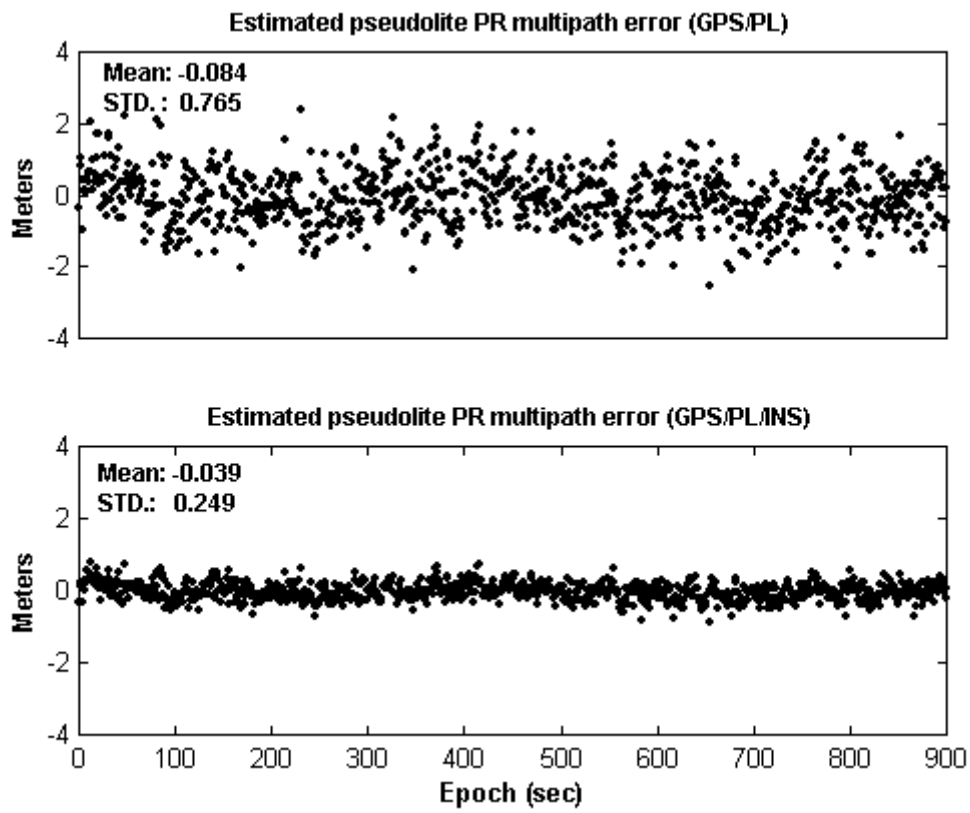


Fig. 10. Pseudolite pseudo-range multipath estimation

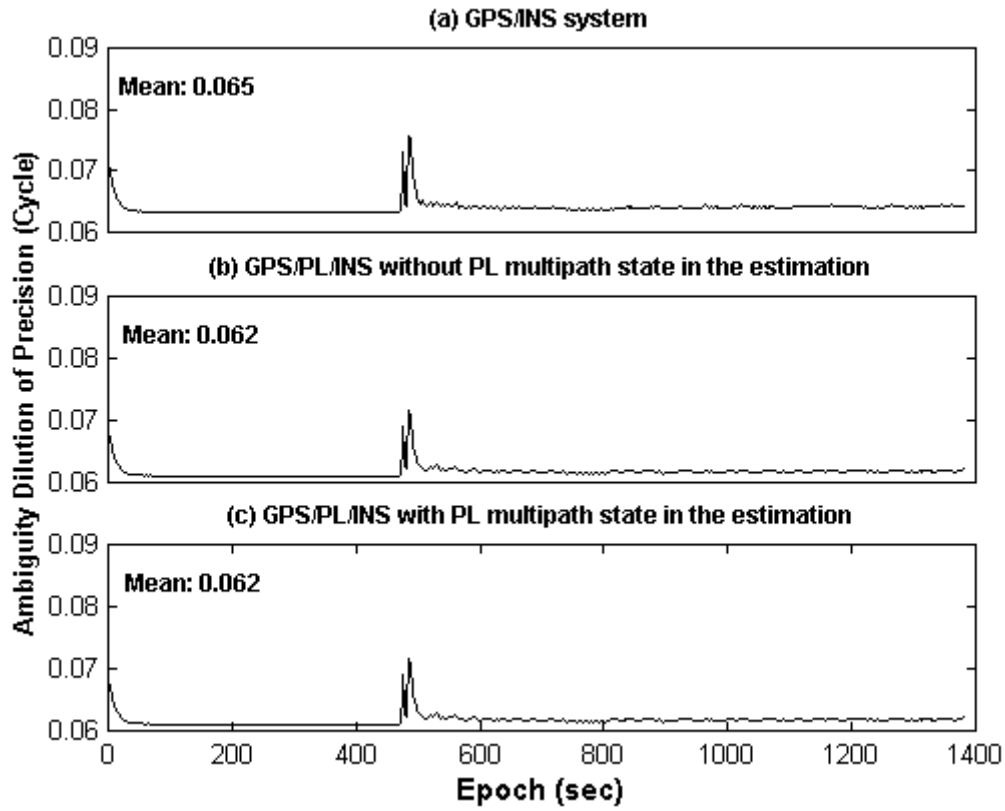


Fig. 11. An effect of including multipath in the pseudolite pseudo-range as an unknown parameter on the float ambiguity estimation

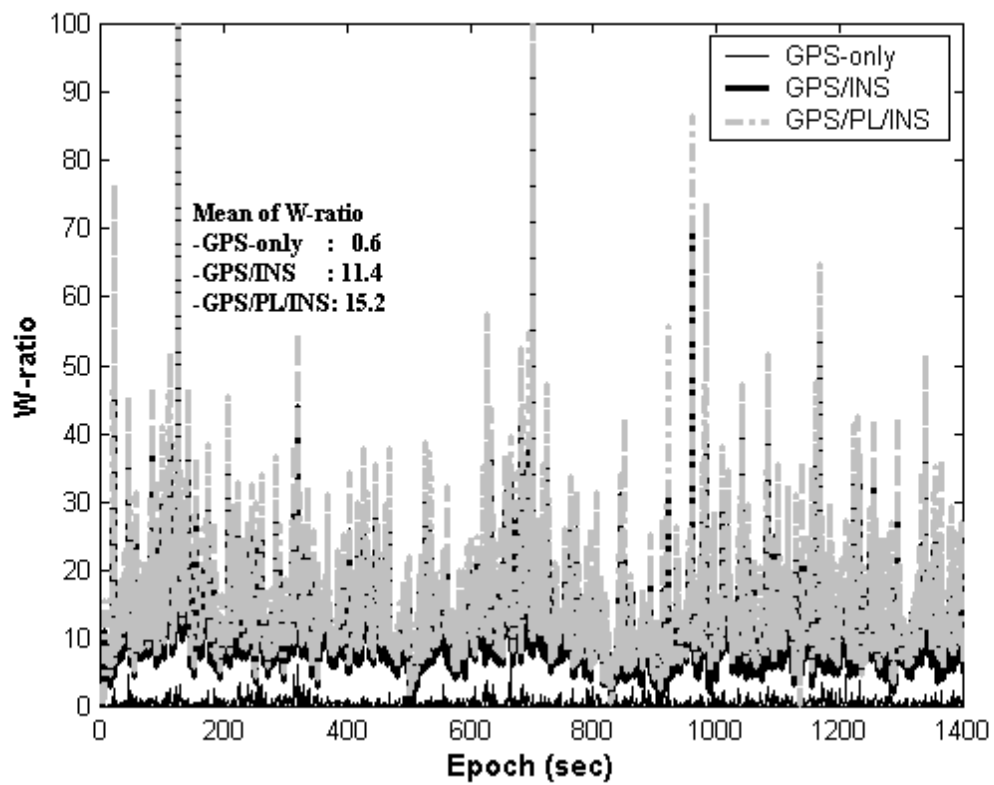


Fig. 12. W-ratio values for the different system configurations (epoch-by-epoch solution)

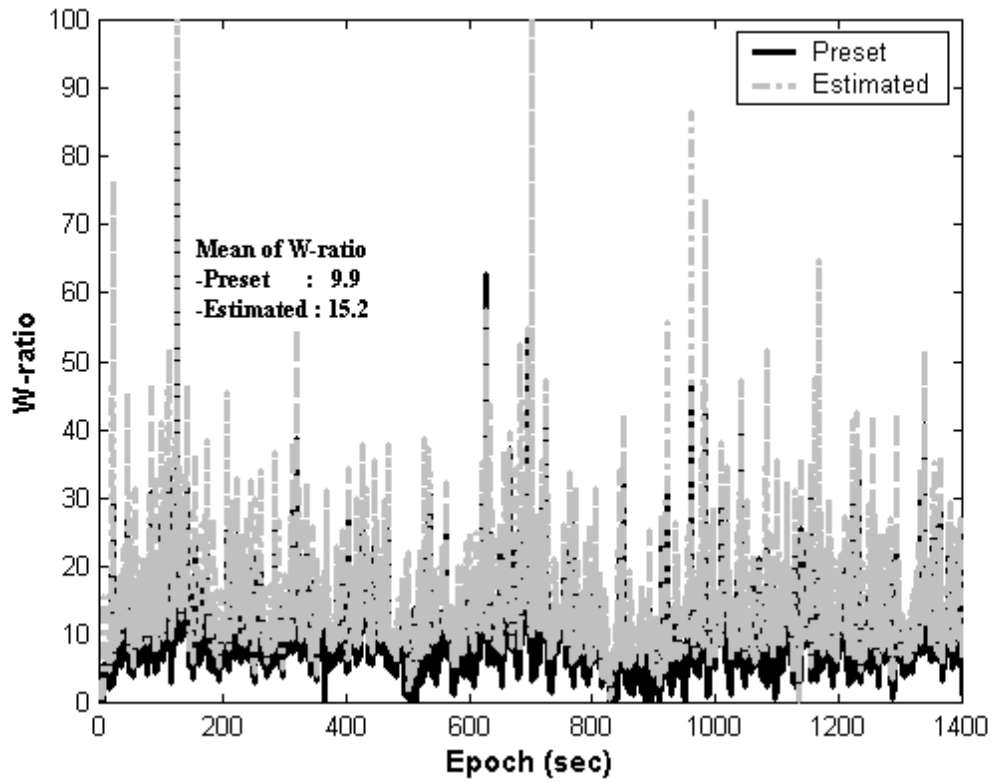


Fig. 13. W-ratio values for the different stochastic models (epoch-by-epoch solution)

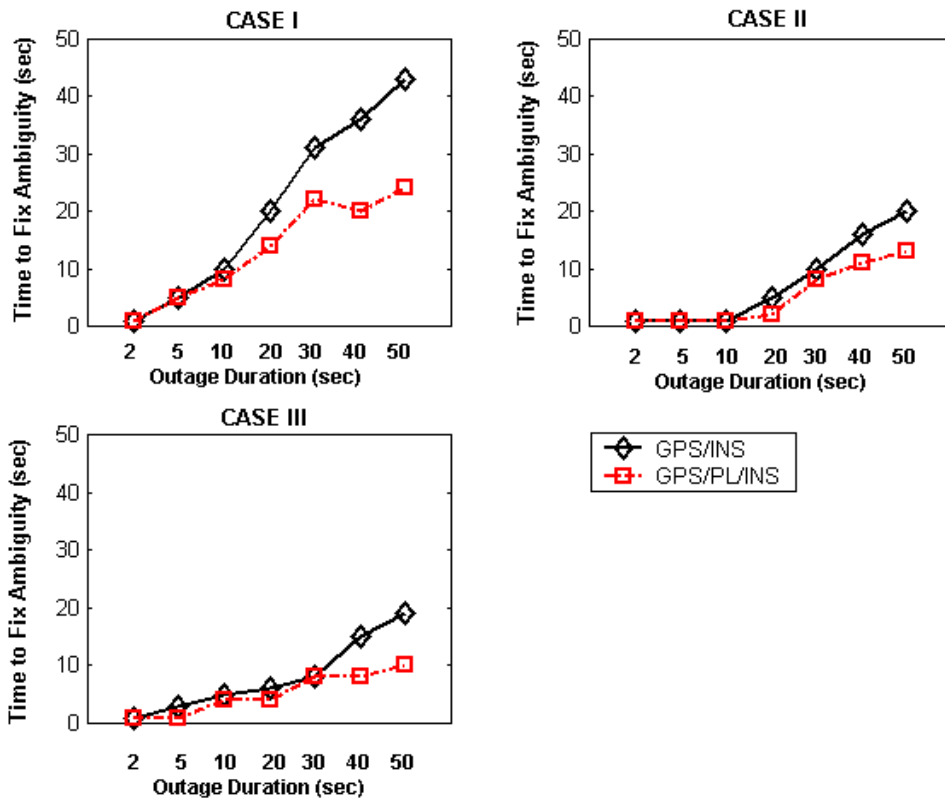


Fig. 14. Time to fix L1 carrier phase ambiguity after different lengths of signal blockage